Function principle of a relaxation oscillator based on a bistable quantum Hall device

G. Nachtwei,[a)] N. G. Kalugin, B. E. Sağol, and Ch. Stellmach
Institut für Technische Physik, Technische Universität Braunschweig, Mendelssohnstrasse 2, D-38106 Braunschweig, Germany

G. Hein
Physikalisch-Technische Bundesanstalt, Bundesallee 100, D-38116 Braunschweig, Germany

(Received 12 November 2002; accepted 29 January 2003)

We present a simple relaxation oscillator based on a quantum Hall device with Corbino geometry near the breakdown of the quantum Hall effect. In the hysteresis region of the breakdown, the quantum Hall device exhibits bistable behavior. If a resistance is connected in series and a capacitor in parallel to the quantum Hall device, the bistable switching leads to subsequent charging and discharging of the capacitor, detectable as relaxation oscillations. We explain the observed oscillations by solving Kirchhoff's equations and obtain a good quantitative description of the experiment. From this, we deduce some dynamical parameters of the Corbino device and discuss the performance limits of the oscillator.
[DOI: 10.1063/1.1563729]

Various nonlinear electronic devices have been applied for the generation of anharmonic electrical oscillations for a long time, as for example, the use of discharge tubes by Van der Pol and Van der Mark in 1927.[1] The study of such systems is interesting not only from a fundamental point of view[2] (for the understanding of nonlinear phenomena, anharmonic oscillators, and chaos), but also because of applicative aspects. In particular, high-frequency signal generation and processing is of increasing importance with the development of communication technologies, data processing, and optoelectronics. The essential feature of a nonlinear electronic device used for the generation of anharmonic oscillations is its negative differential resistance [a typical example is the resonant tunneling diode (see e.g., Ref. 3)]. Similarly, the unstable behavior of devices showing the quantum Hall effect[4] (QHE) near the breakdown of the QHE was suggested to be used to generate anharmonic oscillations.[5] The instability manifests itself in a hysteresis of the current–voltage curve near the breakdown, as reported early after the QHE discovery[6,7] (for an overview, see the review in Ref. 8 and references therein).

In this letter, we present a relaxation oscillator based on the bistable switching of a QH device with Corbino geometry.[9] Such a device shows an almost ideal insulating behavior in the QH regime until a certain, critical value V_{max} of the source–drain voltage V_{SD}. At V_{max}, a sudden onset of the source-drain current I_{SD} occurs. A subsequent reduction of V_{SD} leads to sudden interrupt of I_{SD} at another critical voltage V_{min} ($V_{min}<V_{max}$). In the hysteresis region $V_{min}<V_{SD}<V_{max}$, the QH device exhibits bistable behavior. If a resistance is connected in series and a capacitor as an accumulating device in parallel to the QH device, the bistable switching leads to subsequent charging and discharging of the capacitor, detectable as relaxation oscillations. We explain the observed oscillations by solving Kirchhoff's equations of the circuitry and obtain a good quantitative agreement with the experiment. The model allows us to calculate the dependence of the oscillation frequency on the driving voltage and the circuit parameters. From this, we are able to deduce dynamical parameters of the Corbino device and to discuss the possible limits (e.g., the frequency limit) of the oscillator.

We have patterned circular Corbino devices (radii of inner and outer contacts 100 and 300 μm, respectively) on a GaAs/GaAlAs heterostructure wafer with an electron density of $n_s=2.9\times10^{11}\ \mathrm{cm}^{-2}$ and a Hall mobility of $\mu_H=1\times10^5\ \mathrm{cm}^2/\mathrm{V\,s}$. The sample properties n_s and μ_H were deduced from Shubnikov–de Haas oscillations (Fig. 1), and the QH-breakdown properties from the $I-V$ characteristics [source-drain current I_{SD} versus source–drain voltage V_{SD} (see inset of Fig. 1)].

From the inset of Fig. 1, the hysteresis of the QH breakdown with respect to the critical source–drain voltage is clearly visible. The corresponding bistable region of the $I-V$ curve is exploited for our oscillator. The scheme of the os-

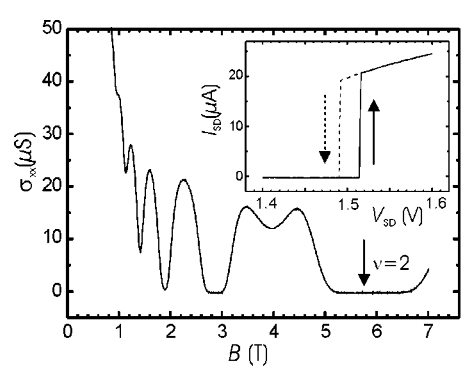

FIG. 1. Shubnikov–de Haas oscillations (dc measurement of $\sigma_{xx}(B)$ at $V_{SD}=100$ mV) of the QH Corbino device. Inset: Current–voltage characteristics of the Corbino sample at $B=5.7$ T (second QH plateau).

[a)]Electronic mail: g.nachtwei@tu-bs.de

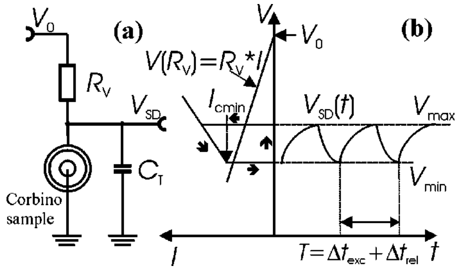

FIG. 2. (a) Scheme of the oscillator circuit. R_V is the serial resistance, C_T is the total capacitance of the circuit. (b) Function principle of the oscillator. For an appropriate choice of R_V and the driving voltage V_0, oscillations of the voltage V_{SD} at the Corbino device occur between the dynamical hysteresis limits V_{min} and V_{max}.

cillator circuit and the function principle are sketched in Figs. 2(a) and 2(b). The total capacitance (capacitor C_T) is charged via the serial resistor R_V, until the breakdown voltage V_{max} (upsweep) is reached. During this process, the Corbino device is insulating and acts like an open switch. The voltage V_{max} closes the switch, and C_T starts to discharge via the Corbino device, which has now a finite resistance R_{CB}. This process endures until the voltage falls to V_{min}, at which the Corbino device becomes insulating again. Thus, the oscillation amplitude ΔV is determined by the hysteresis, $\Delta V = V_{max} - V_{min}$.

From Fig. 2(b), it can be seen that there is a certain range for the choice of the driving voltage V_0 and the serial resistor R_V to keep the oscillator inside the working regime: (a) the current through R_V for the Corbino device being at V_{min} must not exceed the limit $I_c^{min} = V_{min}/R_{CB}$ (for $V_0 - V_{min} \geqslant R_V \cdot I_c^{min}$, a stable solution exists on the resistive branch of the $I-V$ curve of the QH device, corresponding to a stationary state without oscillations); and (b) the driving voltage must be $V_0 > V_{max}$.

From conditions (a) and (b), it can be concluded that the lower limit for the serial resistance value is $R_V > \Delta V / I_c^{min}$. Once R_V is chosen, the choice determines the operational range for the driving voltage V_0 according to conditions (a) and (b):

$$V_{max} < V_0 < V_{min} \cdot \frac{R_{CB} + R_V}{R_{CB}}. \quad (1)$$

The time constants τ_{exc} and τ_{rel}, as well as the voltage V_{SD} at the Corbino device, for the charging and discharging processes, can be determined from the solutions of Kirchhoff's equations with an open switch and R_{CB}, respectively. This yields (akin to the results for relaxation oscillators based on tunnel diode circuits[10]) exponential time dependences for the charging with $\tau_{exc} = R_V C_T$, and with $\tau_{rel} = R_{CB} R_V C_T / (R_{CB} + R_V)$ for the discharging, where R_V and R_{CB} act as parallel resistors. The oscillation period $T = \Delta t_{exc} + \Delta t_{rel}$ is determined not only by τ_{exc} and τ_{rel}, but also by the hysteresis limits V_{max} and V_{min}, and by the driving voltage V_0:

$$T = \tau_{exc} \ln\left(\frac{V_0 - V_{min}}{V_0 - V_{max}}\right) + \tau_{rel} \ln\left(\frac{V_{max} - \Theta V_0}{V_{min} - \Theta V_0}\right), \quad (2)$$

where $\Theta = R_{CB}/(R_{CB} + R_V)$. With increasing driving voltage V_0, the charging time Δt_{exc} decreases and the discharging time Δt_{rel} increases [for V_0 in the operation interval as given in Eq. (1)]. The oscillation frequency f as a function of V_0 has a maximum value at

$$V_0(f_{max}) = \frac{V_{min} V_{max}}{V_{min} + V_{max}} \left(2 + \frac{R_V}{R_{CB}}\right). \quad (3)$$

At V_0 (f_{max}), the oscillator frequency can exceed the value $f = (\tau_{exc} + \tau_{rel})^{-1}$ considerably.

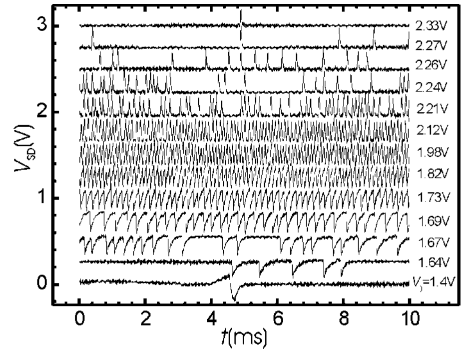

FIG. 3. Relaxation oscillations of the Corbino oscillator at different driving voltages V_0 (curves shifted for clarity). The oscillator operates at V_0 between 1.65 and 2.25 V. Whereas the oscillation amplitude is almost constant within this range, the frequency changes, and has a maximum at $V_0 \approx 2$ V.

Figure 3 shows a set of measured oscillation curves $V_{SD}(t)$ for various values of the driving voltage V_0. To ensure the working regime of the oscillator, we have chosen a serial resistor $R_V = 46$ kΩ of comparable size with the dissipative Corbino resistance $R_{CB} = 76$ kΩ. From the $I-V$ curve (inset of Fig. 1) and Eq. (1), this would yield an operation interval for V_0 from 1.52 to 2.39 V. As seen from Fig. 3, the oscillator works within about 1.65 V $< V_0 <$ 2.25 V, an interval which is distinctively narrower than the one deduced from the dc-measured hysteresis of the $I-V$ curve. In turn, the amplitude is larger than ΔV taken from Fig. 1. Both discrepancies can be resolved simultaneously taking into account a wider dynamical hysteresis at the oscillator frequencies of some kilohertz in comparison to the quasistationary one. Therefore, we have supplemented the dc-measurement of the hysteresis by ac data in the frequency range from $0 < f \leqslant 10$ kHz. We observed a *drastic increase of the hysteresis* at low frequencies (from 25 mV at dc to 0.4 V at 27 Hz), and a saturation at higher frequencies (0.3 V–0.4 V for f from 100 Hz to 1 kHz). The occurrence of a hysteresis in the $I-V$ characteristics of QH samples near the breakdown is commonly explained on the basis of an electron heating model (see, e.g., Refs. 6, 11, 12). The hysteresis is mainly determined by the contribution of hopping processes between localized states to the conduction.[12] Applying this model to our sample, a suppression of the hopping contribution from $\sigma_{hop} = 1.3 \times 10^{-3}\, \sigma_{xy}$ at dc to $\sigma_{hop} = 4.5 \times 10^{-4}\, \sigma_{xy}$ ($\sigma_{xy} = 77.481\ \mu$S for the second QH plateau) at $f = 27$ Hz can explain the observed increase of the hysteresis.[13] A reduction of the hopping conductivity corresponds to a shrinking of the localization length[14] with increasing frequency. The measured oscillation amplitude is a direct measure of the dynamical hysteresis of the QHE breakdown at the oscillation frequency. Therefore, the oscillator provides access to determine the breakdown properties at higher frequencies.

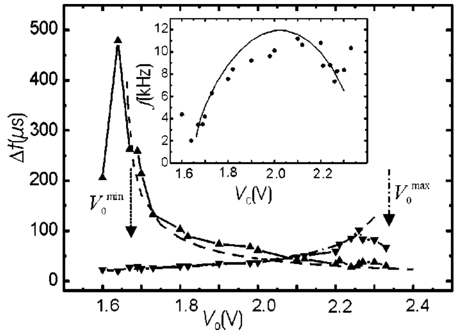

FIG. 4. Measured charging times Δt_{exc} (up triangle) and discharging times Δt_{rel} (down triangle) as a function of the driving voltage V_0, in comparison to the calculated values (dashed line: charging, dash-dotted line: discharging) with the parameters $\tau_{exc}=96\ \mu s$, $\tau_{rel}=60\ \mu s$, $V_{min}=1.46$ V, $V_{max}=1.66$ V. The limits of the working regime as calculated from the model are depicted by arrows. Inset: Oscillator frequency f as a function of the driving voltage V_0 (• measured values, solid line: model).

The amplitude of the oscillations remained almost unchanged (from 180 to 250 mV) with V_0 in the working regime (close to the operation limits of the oscillator, the amplitudes tend to vary). The measured charging and discharging times show a pronounced V_0-dependence, which we used to estimate the total capacitance C_T of the circuit. To reach higher frequencies, no separate capacitor was attached, so that C_T is dominated by the capacitance of cables and connectors [for C_T, the capacitances of the Corbino device (<0.1 pF) and of the input of the oscilloscope (20 pF) can be neglected]. From the measured values of Δt_{exc} and Δt_{rel} as a function of V_0, the best fit applying Eq. (4) was obtained with $C_T=2.1$ nF. Figure 4 presents the corresponding data in comparison to the calculated dependences. The measured dependences of Δt_{exc} and Δt_{rel} on V_0 are reproduced quite well, including the operation range of the oscillator. The calculations yield a maximum oscillation frequency of 11.9 kHz at $V_0=2.02$ V, which is in reasonable agreement with the experimental value of $f_{max}=11.2$ kHz at $V_0=2.1$ V (see inset of Fig. 4).

The upper frequency of the oscillator is determined mainly by the capacitance C_T and the serial resistance R_V. The dissipative resistance of the Corbino device R_{CB} is of less importance, as it acts only as a parallel shunt to R_V for the discharging process. Consequently, to reach higher frequencies, the values of C_T and R_V should be reduced. Smaller R_V values require, according to $R_V^{min}=\Delta V/I_c^{min}$, a reduced hysteresis. Thus, higher frequencies can be realized only by a simultaneous reduction of the oscillation amplitude. The physical limits of the oscillation frequency are given by the switching times of the Corbino device, which we have found to be rather short (a few nanoseconds in low-mobility samples[9]). With this, upper frequencies in the gigahertz range are potentially accessible. Of course, there are simpler solutions to generate gigahertz oscillations, such as, for example, resonant tunneling devices.[3] However, although the Corbino oscillator is only of limited value for VHF applications, it provides additional insight into the dynamical properties of the breakdown of the QHE (dynamical hysteresis).

To summarize, we have generated relaxation oscillations applying a quantum Hall Corbino device as bistable switching element. The oscillation amplitude is determined by the dynamical hysteresis of the QH device. The frequency of the oscillation depends not only on the resistances and capacitances of the circuit, but also on the dynamical hysteresis of the Corbino device. This hysteresis is determined by the dynamical breakdown properties of the device and can be directly deduced from the measurements. The hysteresis already exhibits a strong increase at low frequencies, which is explained by a reduced hopping contribution to the conductivity σ_{xx}. With knowledge of the limiting voltages of the dynamical hysteresis and of the resistances and capacitances of the circuit, the properties of the oscillator, as, for example the frequency as a function of the driving voltage, can be modeled in good agreement with the experiment. The highest frequencies are achievable by the application of QH devices with a small, but stable dynamical hysteresis in the $I-V$ characteristics of the breakdown.

We would like to thank Dr. K. Eberl for providing the GaAs/GaAlAs wafer. This study was supported by the Deutsche Forschungsgemeinschaft (DFG, project Na235/10-2). One of the authors (B.E.S.) acknowledges support by the Deutscher Akademischer Austauschdienst (DAAD).

[1] B. Van der Pol and J. Van der Mark, Nature (London) **120**, 363 (1927).
[2] A. A. Andronov, A. A. Vitt, and S. E. Khaikin, *Theory of Oscillators* (Pergamon, New York, 1966).
[3] E. R. Brown, J. R. Söderström, C. D. Parker, L. J. Mahoney, K. M. Molvar, and T. C. McGill, Appl. Phys. Lett. **58**, 2291 (1991).
[4] K. von Klitzing, G. Dorda, and M. Pepper, Phys. Rev. Lett. **45**, 494 (1980).
[5] The application of a Corbino device near the breakdown of the QHE for generating oscillations was proposed by N. G. Kalugin (unpublished, 2002).
[6] G. Ebert, K. von Klitzing, K. Ploog, and G. Weimann, J. Phys. C **16**, 5441 (1983).
[7] M. E. Cage, R. F. Dziuba, B. F. Field, E. R. Williams, S. M. Girvin, A. C. Gossard, D. C. Tsui, and R. J. Wagner, Phys. Rev. Lett. **51**, 1374 (1983).
[8] G. Nachtwei, Physica E (Amsterdam) **4**, 79 (1999).
[9] B. E. Sağol, G. Nachtwei, K. von Klitzing, G. Hein, and K. Eberl, Phys. Rev. B **66**, 075305 (2002).
[10] W. F. Chow, *Principles of Tunnel Diode Circuits* (Wiley, New York, 1964).
[11] S. Komiyama, T. Takamasu, S. Hiyamizu, and S. Sasa, Solid State Commun. **54**, 479 (1985).
[12] G. Nachtwei, Z. H. Liu, G. Lütjering, R. R. Gerhardts, D. Weiss, K. von Klitzing, and K. Eberl, Phys. Rev. B **57**, 9937 (1998).
[13] The detailed description of the measurements and model calculations of the breakdown hysteresis in Corbino devices is in preparation for a subsequent publication.
[14] F. Hohls, U. Zeitler, and R. J. Haug, Phys. Rev. Lett. **88**, 036802 (2002).